IEEE Access
Multidisciplinary | Rapid Review | Open Access Journal

Received 16 June 2022, accepted 27 June 2022, date of publication 5 July 2022, date of current version 11 July 2022.

Digital Object Identifier 10.1109/ACCESS.2022.3188719

RESEARCH ARTICLE

A Novel Event-Triggered Control of DC Microgrids Against Probabilistic Actuator Fault

BOWEI JI, ZHOU GU, (Member, IEEE), AND XIUFENG MU
College of Mechanical and Electronic Engineering, Nanjing Forestry University, Nanjing 210037, China

Corresponding author: Zhou Gu (gzh1808@163.com)

This work was supported by the National Natural Science Foundation of China under Grant 6210021545.

ABSTRACT This article investigates a problem of event-triggered controller design for DC microgrid, in which multiple nonlinear Constant power loads (CPLs) and probabilistic actuator fault are considered. A novel pre-averaged event-triggered mechanism (PAETM) is put forward, under which the average value of each time interval is used to determine the triggering instead of using the sample data that represents the system characteristic partially. Benefit from this mechanism, triggering events are reduced and the network burden is mitigated while the system performance is ensured, which contributes to a higher efficiency for DC microgrid. Considering various disturbances in DC microgrid, a unified PAETM controller design for DC microgrid with probabilistic distribution actuator fault and disturbance is proposed. Finally, a simulation example is shown to illustrate the validity of the proposed control strategy.

INDEX TERMS DC microgrid, pre-averaged event-triggered mechanism (PAETM), constant power load, actuator fault.

I. INTRODUCTION

As renewable energy develops, DC microgrids as a novel form of power system containing generators, loads, and energy storage have aroused extensive attention in both academic and industrial field [1]. DC microgrids demonstrate multiple superiorities for having higher efficiency and reliability, simpler control design procedure, and a more natural interface for various energy storage systems (ESSs) and loads, because of that, microgrids draws multi studies such as [2]–[4]. Hence, the stability and stabilization of DC microgrids are significant to be addressed.

Constant power loads (CPLs), which are modeled by loads in DC microgrids have some undesired effects, like exhibiting negative impedance characteristics [5] that may increase the nonlinearity degree of the system or even destabilize the overall system [6]. Several methods have been proposed to alleviate the negative effects, which can be sketchily separated into two types: the passive damping way and the active damping way. The passive damping way is mostly achieved by adding a series of capacitors [7], which is limited because of low efficiency and its physical constraints. On the other side, the active damping way mainly focuses on the modification of the control loop [8], [9]. In [10], the control loop is modified to increase the damping of passive elements. However, this kind of method may experience side effects such as transient oscillation or loads damage. For this reason, the method of using injecting current to stabilize the DC microgrids is proposed, which includes linear and nonlinear approaches in general. The linear approach like [11], is achieved by taking the nonlinearity of CPLs out of consideration. The nonlinear methods of backstepping [5], [12], sliding mode [13], and robust control [14] are adopted to obtain certain effects. Yet it should be noticed that DC microgrids are mostly distributed, and the constituents of DC microgrids may spatially separate far from each other, which means the control signal and system information will be needed to be transmitted through the network environment and certain communicating schemes needed to be considered [1], [15].

Introducing network as a communication medium of DC microgrids brings various advantages such as higher efficiency and reliability. While making DC microgrids much

The associate editor coordinating the review of this manuscript and approving it for publication was Engang Tian.

more intelligent, the involvement of the network also brings challenges and problems. Communication structure needs to be designed, and certain performances caused by network that may destabilize the system need to be further investigated. Firstly, there are generally three communication structures: centralized structure [16], distributed structure [17], [18], and decentralized structure [1]. A centralized structure for its efficiency and realizability is utilized in this paper, which is achieved by gathering the information of each unit in the center controller to generate control signal. Secondly, the problems induced by the network mainly are network-induced delay and packet drops [19]. Also, the limitation of bandwidth as an inherent property of network that inevitably influences system performance must be considered which is not fully covered in the aforementioned results.

To cope with the network limitation, an alternative of periodic communication can be realized by ETM [20]. The ETM is designed by replacing the determination of whether the control signal need to be sent to a predefined event-triggered condition. This means the control signal will only be sent when the triggered condition is violated, saving network resources efficiently. Plenty of results like [21]–[23] indicate that ETM can save communication resources while retain the system performance in an acceptable range. Event-triggering control as a widely investigated subject in recent years has expanded in various forms [24]–[29]. In [27], an event-triggered tracking controller was proposed, and battery energy storage system control involving event-triggering is mentioned in [28]. For DC microgrids, authors in [30] presented an adaptive triggered controller while model uncertainties are considered. An event-triggered communication-based dynamic consensus algorithm was proposed in [31] to achieve both proportional current sharing and DC voltage regulation. And [32] proposed a novel form of the event triggering control by designing triggering conditions under super twisting reaching law. Meanwhile, the event-triggered control itself has expanded many varieties in development, such as the self-triggered control (STC) [33], [34], which predicted the next event instant based on the historical information and system knowledge, and dynamical event-triggering like [27], [35], [36], which adds more flexibility items to the event-triggered control. However, the DC microgrid system can be affected easily by various physical reasons, which cause many extra triggering events when applying traditional ETM. Those extra triggering events increase the network burden and cause energy-wasting, which motivates the present work.

In this work, to stabilize the disturbed DC microgrid while reducing the unnecessary triggering events, a novel event-triggered controller is proposed. The main contributions are as follows:

1) A novel PAETM for nonlinear DC microgrid system is proposed by replacing the conventional sampled data in ETM with average data, which contains the system information in each certain time interval and better represents the trend of the system. The proposed PAETM effectively reduces the triggering events cause by disturbance, and mitigates the network burden and raises efficiency while ensuring system performance.
2) A new event-triggered control strategy is developed for nonlinear DC microgrid. Compared with the existing literatures, the probabilistic fault and external disturbance are considered in this research, which better reflect the actual interference experienced in DC microgrid. The use of this control strategy brings the lower consumption and higher efficiency of DC microgrid.

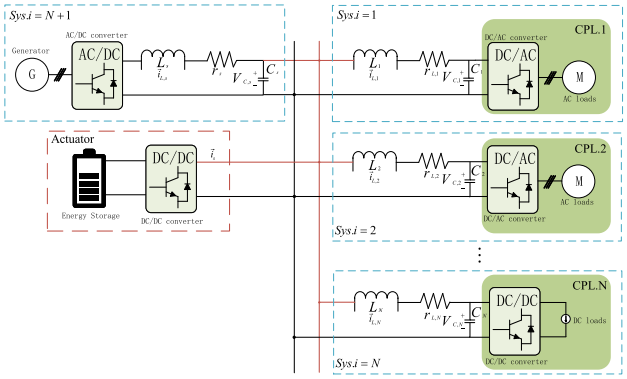

FIGURE 1. Circuit diagram.

II. PROBLEM FORMULATION

A. SYSTEM DESCRIPTION

The structure of the DC microgrid with CPLs is depicted in Fig. 1. The basic physical variables of the DC microgrid is denoted the same as [37] for a convenience purpose. The microgrid is formed by $N+1$ subsystems containing N CPLs and one ESS. By define the system state variable as $\tilde{x}_i(t) = [i_{L,i} \quad v_{C,i}]^T$, $\tilde{x}_s = [i_{L,s} \quad v_{C,s}]^T$. The state equation of ith CPL subsystem is considered as follows:

$$\dot{\tilde{x}}_i(t) = \mathcal{A}_i\tilde{x}_i(t) + f_i\upsilon_i(\tilde{x}_i(t)) + \mathcal{A}_{is}\tilde{x}_s(t), \tag{1}$$

where

$$\mathcal{A}_i = \begin{bmatrix} -\frac{r_{L,i}}{L_i} & -\frac{1}{L_i} \\ \frac{1}{C_i} & 0 \end{bmatrix}, f_i = \begin{bmatrix} 0 \\ \frac{1}{C_i} \end{bmatrix},$$
$$\mathcal{A}_{is} = \begin{bmatrix} 0 & \frac{1}{L_i} \\ 0 & 0 \end{bmatrix}, \upsilon_i(\tilde{x}_i(t)) = \frac{P_i}{v_{c,i}},$$
$$i = \{1, 2, \cdots, N\}, s = N+1.$$

Assuming that all the CPLs and powers are ideal and consider the current of ESS i_{es} as the control signal u. The state equation of DC source are as follows:

$$\dot{\tilde{x}}_s(t) = \mathcal{A}_s\tilde{x}_s(t) + bV_{dc} + b_u u(t) + \sum_{i=1}^{N} \kappa\tilde{x}_i(t), \tag{2}$$

where

$$\mathcal{A}_s = \begin{bmatrix} -\frac{r_s}{L_s} & -\frac{1}{L_s} \\ \frac{1}{C_s} & 0 \end{bmatrix}, b = \begin{bmatrix} \frac{1}{L_s} \\ 0 \end{bmatrix},$$
$$\kappa = \begin{bmatrix} 0 & 0 \\ -\frac{1}{C_s} & 0 \end{bmatrix}, b_u = \begin{bmatrix} 0 \\ -\frac{1}{C_s} \end{bmatrix}.$$

For the concise purpose the equilibrium point is shifted to origin by coordinate transformation. Augmenting the CPLs (1) and the ESS (2), and taking the external disturbance $\varrho(t) \in L_2[0, \infty)$ with appropriate dimension matrix $\mathcal{W}$ into consideration, the state equation of the system is rewritten as:

$$\dot{x}(t) = \mathcal{A}x(t) + F\Upsilon(x(t)) + \mathcal{B}_u u(t) + \mathcal{W}\varrho(t), \tag{3}$$

where

$$x(t) = [x_1^T(t), x_2^T(t), \cdots, x_N^T(t), x_s^T(t)]^T = \tilde{x}(t) - x_e,$$
$$\Upsilon(x(t)) = [\upsilon_1(x_1(t)), \upsilon_2(x_2(t)), \cdots, \upsilon_N(x_N(t))]^T,$$
$$\mathcal{A} = \begin{bmatrix} \mathcal{A}_1 & 0 & \cdots & 0 & \mathcal{A}_{1s} \\ 0 & \mathcal{A}_2 & \cdots & 0 & \mathcal{A}_{2s} \\ \vdots & \vdots & \ddots & \vdots & \vdots \\ 0 & 0 & \cdots & \mathcal{A}_N & \mathcal{A}_{Ns} \\ \kappa & \kappa & \cdots & \kappa & \mathcal{A}_s \end{bmatrix},$$
$$F = \begin{bmatrix} f_1 & 0 & \cdots & 0 \\ 0 & f_2 & \cdots & 0 \\ \vdots & \vdots & \ddots & \vdots \\ 0 & 0 & \cdots & f_N \\ 0 & 0 & \cdots & 0 \end{bmatrix}, \mathcal{B}_u = \begin{bmatrix} 0 \\ \vdots \\ 0 \\ b_u \end{bmatrix},$$

and

$$\upsilon_i(x_i^T(t)) = \frac{P_i v_{C,i}}{v_{c0,i}(v_{C,i} + v_{c0,i})}, \tag{4}$$

in which x_e and $v_{c0,i}$ represent the equilibrium point of DC microgrid.

The nonlinear vector $\Upsilon(x(t))$ in the DC microgrid system (3) satisfies:

$$\Upsilon^T(x(t))\Upsilon(x(t)) = \sum_{i=1}^{N} \upsilon_i^T(x_i(t))\upsilon_i(x_i(t)) \leq \alpha^2 x^T(t)\mathcal{H}^T\mathcal{H}x(t), \tag{5}$$

where α is the robustness index, and the matrix $\mathcal{H}$ is

$$\mathcal{H} = \begin{bmatrix} h & \cdots & 0 & 0 \\ \vdots & \ddots & \vdots & \vdots \\ 0 & \cdots & h_N & 0 \\ 0 & \cdots & 0 & 0 \end{bmatrix}, h_j = \begin{bmatrix} 0 & 0 \\ 0 & 1 \end{bmatrix}, i \in 1, 2, \cdots, N.$$

B. NOVEL EVENT-TRIGGERED SCHEME AND CONTROLLER DESIGN

The PAETM and the controller design will be developed in this part. An averaging mechanism is added to the system before the sampling as Fig. 2 shows, which aims to achieve better performance. The averaging mechanism is designed as

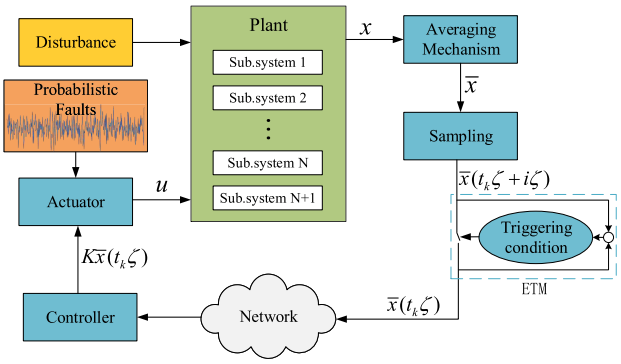

FIGURE 2. System structure.

$$\bar{x}(t) = \frac{1}{\mathcal{T}} \int_{t-\mathcal{T}}^{t} x(s)ds, \tag{6}$$

where $\mathcal{T}$ denotes for the averaging period. The average mechanism (6) satisfies:

$$\frac{1}{\mathcal{T}} \int_{t-\mathcal{T}}^{t} x(s)ds \approx \frac{1}{6}[x(t) + 4x(t - \frac{\mathcal{T}}{2}) + x(t - \mathcal{T})]. \tag{7}$$

Remark 1: The average value of each time interval $\mathcal{T}$ is sampled, and used to decide whether the system information is needed for stabilization. Under the traditional ETM, the fixed period sampling probably samples during the system jitter and generates sampling data that can not represent the system characteristic accurately. This data causes unnecessary triggering events. It may waste network resources and cause network jams. However, with this improvement, the unnecessary triggering caused by the aforementioned reason can be avoided, and the network resource can be efficiently used.

Remark 2: Notice that the average mechanism (6) is approximated by a time delay polynomials in (7), which makes the unified control design scheme achieved by the time-delay system approach possible.

Based on the averaging mechanism (6) and (7), the injecting current $u(t)$ as the control signal is considered as

$$u(t) = K\bar{x}(t), \tag{8}$$

where K represents the controller needed to be designed.

The injecting current of DC microgrid may experience fluctuation due to the load variation and interference from various reasons. Considering the probabilistic actuator faults, the controller (8) is rewritten as:

$$u(t) = \Lambda K\bar{x}(t) = \sum_{i=1}^{m} \lambda_i \mathcal{C}_i K\bar{x}(t), \tag{9}$$

where $\Lambda = diag\{\lambda_1, \cdots, \lambda_m\}$; $\lambda_i (i = 1, \cdots, m)$ stands for different independent stochastic variables which have

expectation $\bar{\lambda}_i(0 < \bar{\lambda} < \bar{\lambda}_{max})$ and variance β_i^2; $\mathcal{C}_i = diag\{\underbrace{0,\cdots,0}_{i-1},1,\underbrace{0,\cdots,0}_{m-1}\}$.

Remark 3: DC microgrid experiences multiple influences from various sources, such as loads and powers. Therefore, probabilistic actuator fault and external disturbance are considered in this system model.

The release instants are denoted by $t_0\eta, t_1\eta, t_2\eta\cdots$, where $t_0\eta = 0$ is the initial instant, η denotes the sampling interval. By assuming the maximum delay time of the internet is ς_M as a positive real number, the time-varying delay of network ς_k has $\varsigma_k \in [0, \varsigma_M)$. By this, the signal sent at $\{t_0\eta, t_1\eta, t_2\eta, \cdots\}$ will arrived at $\{t_0\eta+\varsigma_0, t_1\eta+\varsigma_1, t_2\eta+\varsigma_2, \cdots\}$, respectively. The definition of the network-induced delay $\varsigma(t)$ and the event triggering error $\delta_k(t)$ is as follows:

$$\varsigma(t) := t - t_k\eta - i\eta, \tag{10}$$

$$\delta_k(t) := \bar{x}(t_k\eta) - \bar{x}(t_k\eta + i\eta), \tag{11}$$

where $t \in \iota_i, i = 0, \ldots, p_k, \varsigma(t) \in [0, \eta + \varsigma_M)$, and

$$\iota_i = \begin{cases} [t_k\eta + \varsigma_k, t_k\eta + \eta + \varsigma_M), & i = 0 \\ [t_k\eta + p_k\eta + \varsigma_M, t_{k+1}\eta + \varsigma_{k+1}), & i = p_k \\ [t_k\eta + i\eta + \varsigma_M, t_k\eta + (i+1)\eta + \varsigma_M), & else \end{cases}$$

Utilizing (7), the triggering condition is designed as

$$\delta_k^T(t)\Omega\delta_k(t) \le \frac{\sigma}{36}m^T(t)\Omega m(t), \tag{12}$$

where

$$m(t) = x(t-\varsigma(t)) + 4x(t-\varsigma(t)-\frac{\mathcal{T}}{2}) + x(t-\varsigma(t)-\mathcal{T}).$$

Then event triggered controller (9) can be expressed as follows by utilizing (10) and (11):

$$u(t) = \Lambda K(\delta(t) + \bar{x}(t-\varsigma(t))). \tag{13}$$

Remark 4: The traditional ETM uses sample data to determine the triggering events and generates control signal. However, the fixed period sampling of this mechanism results in the system information loss between each two sampling instants. To solve this problem, an average value that contains the system information during sample intervals is used in our proposed PAETM, which can better represent the system characteristic. This information is used to decide whether triggering is necessary. This mechanism efficiently avoids the excess triggering events, which reduces the energy consumption and lengthens the operation life of the DC microgrid.

Remark 5: Obviously, the Zeno behavior can be successfully avoided under the proposed PAETM (12).

The dynamic of the DC microgrid (3) can be reconstructed as

$$\begin{aligned}\dot{x}(t) = {} & \mathcal{A}x(t) + F\Upsilon(x(t)) + \mathcal{B}_u(\Lambda - \bar{\Lambda})K(\bar{x}(t-\varsigma(t)) + \delta(t)) \\ & + \mathcal{B}_u\bar{\Lambda}K(\bar{x}(t-\varsigma(t)) + \delta_k(t)) + \mathcal{W}\varrho(t),\end{aligned} \tag{14}$$

where $\bar{\Lambda} = diag\{\bar{\lambda}_1, \cdots, \bar{\lambda}_m\}$.

In this scheme, the feedback gain matrix K in (13) will be designed, which makes the system (14) globally asymptotically stable in mean square sense under the limited network environment.

III. MAIN RESULTS

In this section, based on the system discussed in (14) and the PAETM (12), under a given disturbance attenuation level γ, the state feedback control law will be designed to satisfy the condition $\|x(t)\|_2 \le r\,\|\varrho(t)\|_2$ with $\varrho(t) \in L_2[0,\infty)$.

Theorem 1: For given scalars σ, α, γ and ρ, and gain matrix K, $\lambda_i(i = 1,\cdots,m)$, $\beta_i(i = 1,\cdots,m)$. The DC microgrid system described as (14) is globally asymptotically stable in mean square sense if there exist matrices $P > 0$, $Q > 0, R > 0, \Omega > 0$ and S with appropriate dimensions that

$$\begin{bmatrix}\Xi_{M1} & * \\ \Xi_{M2} & \Xi_{M3}\end{bmatrix} < 0, \tag{15}$$

$$\begin{bmatrix}R & * \\ S & R\end{bmatrix} \ge 0, \tag{16}$$

where

$$\Xi_{M1} = \begin{bmatrix}\Xi_1 & * & * & * \\ \Xi_2 & -\Omega & * & * \\ \Xi_3 & 0 & -Q-R & * \\ \Xi_4 & \sqrt{\varsigma_M}R\mathcal{B}_u\bar{\Lambda}K & 0 & -PR^{-1}P\end{bmatrix},$$

$$\Xi_{M2} = \begin{bmatrix}\Xi_5\ 0\ 0\ 0 \\ \Xi_6\ \theta\ 0\ 0 \\ \Xi_7\ 0\ 0\ 0\end{bmatrix},$$

$$\Xi_{M3} = \begin{bmatrix}-\alpha^{-2}I & * & * \\ 0 & \hat{R} & * \\ 0 & 0 & -I\end{bmatrix},$$

$$\Xi_1 = \begin{bmatrix}\xi_1 & * & * & * & * & * \\ F^TP & -I & * & * & * & * \\ \xi_2 & 0 & \frac{\sigma}{36}\Omega+\nu & * & * & * \\ \xi_3 & 0 & \frac{\sigma}{9}\Omega & \frac{4\sigma}{9}\Omega+\nu & * & * \\ \xi_4 & 0 & \frac{\sigma}{36}\Omega & \frac{\sigma}{9}\Omega & \frac{\sigma}{36}\Omega+\nu & * \\ \mathcal{W}^TP & 0 & 0 & 0 & 0 & -\gamma^2I\end{bmatrix},$$

$$\Xi_2 = \begin{bmatrix}K^T\bar{\Lambda}^T\mathcal{B}_u^TP\ 0\ 0\ 0\ 0\ 0\end{bmatrix},$$

$$\Xi_3 = \begin{bmatrix}-\frac{1}{\varsigma_M}S\ 0\ \frac{1}{\varsigma_M}(R+S)\ \frac{1}{\varsigma_M}(R+S)\ \frac{1}{\varsigma_M}(R+S)\ 0\end{bmatrix},$$

$$\Xi_4 = [\Xi_{41}\quad \Xi_{42}],$$

$$\Xi_{41} = \begin{bmatrix}\sqrt{\varsigma_M}RA\ \sqrt{\varsigma_M}RD\ \frac{1}{6}\sqrt{\varsigma_M}R\mathcal{B}_u\bar{\Lambda}K\end{bmatrix},$$

$$\Xi_{42} = \begin{Bmatrix}\frac{2}{3}\sqrt{\varsigma_M}R\mathcal{B}_u\bar{\Lambda}K\ \frac{1}{6}\sqrt{\varsigma_M}R\mathcal{B}_u\bar{\Lambda}K\ \sqrt{\varsigma_M}R\mathcal{W}\end{Bmatrix},$$

$$\Xi_5 = \begin{bmatrix}\mathcal{H}\ 0\ 0\ 0\ 0\ 0\end{bmatrix},$$

$$\Xi_6 = \begin{bmatrix}0\ 0\ \theta\ \theta\ \theta\ 0\end{bmatrix},$$

$$\Xi_7 = \begin{bmatrix}I\ 0\ 0\ 0\ 0\ 0\end{bmatrix},$$

$$\xi_1 = \mathcal{A}^TP + P\mathcal{A} + Q - \frac{1}{\varsigma_M}R,$$

$$\xi_2 = \frac{1}{6}K^T\bar{\Lambda}^T\mathcal{B}_u^TP + \frac{1}{\varsigma_M}(R+S),$$

$$\xi_3 = \frac{2}{3}K^T\bar{\Lambda}^T\mathcal{B}_u^TP + \frac{1}{\varsigma_M}(R+S),$$

$$\xi_4 = \frac{1}{6}K^T\bar{\Lambda}^T\mathcal{B}_u^T P + \frac{1}{\varsigma_M}(R+S),$$
$$\nu = \frac{1}{\varsigma_M}(-2R-S-S^T),$$
$$\theta = [\beta_1 RB\mathcal{C}_1 K, \beta_2 RB\mathcal{C}_2 K, \cdots, \beta_m RB\mathcal{C}_m K]^T,$$
$$\hat{R} = diag\{\underbrace{R, \cdots, R}_{m}\}.$$

Proof: Choose the following Lyapunov functional as

$$V(t) = x^T(t)Px(t) + \int_{t-\varsigma_M}^{t} x^T(s)Qx(s)ds + \int_{t-\varsigma_M}^{t}\int_{s}^{t}\dot{x}^T(v)R\dot{x}(v)dvds. \quad (17)$$

Definition (9) leads to $\bar{\Lambda} = \mathcal{E}\{\Lambda\}$. Then we can get

$$\mathcal{E}\{\Lambda - \bar{\Lambda}\} = 0, \quad (18)$$

where $\mathcal{E}\{\cdot\}$ stands for expectation. Take the expectation of the derivative of V(t) yields:

$$\begin{aligned}\mathcal{E}\{\dot{V}(t)\} &= \mathcal{E}\{2\dot{x}^T(t)Px(t) + x^T(t)Qx(t) \\ &\quad -x^T(t-\varsigma_M)Qx(t-\varsigma_M) \\ &\quad +\varsigma_M\dot{x}(t)R\dot{x} - \int_{t-\varsigma_M}^{t}\dot{x}^T(s)R\dot{x}(s)ds\} \\ &= \mathcal{E}\{2[x^T(t)\mathcal{A}^T Px(t) + \Upsilon^T(x(t))F^T Px(t) \\ &\quad +\frac{1}{6}x^T(t-\varsigma(t)-\mathcal{T})K^T\bar{\Lambda}^T\mathcal{B}_u^T Px(t) \\ &\quad +\frac{2}{3}x^T(t-\varsigma(t)-\frac{\mathcal{T}}{2})K^T\bar{\Lambda}^T B^T Px(t) \\ &\quad +\frac{1}{6}x^T(t-\varsigma(t))K^T\bar{\Lambda}^T\mathcal{B}_u^T Px(t) \\ &\quad +\delta^T(t)K^T\bar{\Lambda}^T\mathcal{B}_u^T Px(t) + \varrho^T(t)\mathcal{W}^T Px(t)] \\ &\quad +x^T(t)Qx(t) - x^T(t-\varsigma_M)Qx(t-\varsigma_M) \\ &\quad +\varsigma_M\dot{x}^T(t)R\dot{x}(t) - \int_{t-\varsigma_M}^{t}\dot{x}^T(s)R\dot{x}(s)ds\}, \quad (19)\end{aligned}$$

where

$$\begin{aligned}\mathcal{E}\{\dot{x}^T(t)R\dot{x}(t)\} &= \mathcal{E}\{(\mathcal{A}x(t) + F\Upsilon(x(t)) + \frac{1}{6}\mathcal{B}_u\bar{\Lambda}Km(t) \\ &\quad +\mathcal{B}_u\bar{\Lambda}K\delta(t) + \mathcal{W}\varrho(t))R(\mathcal{A}x(t) \\ &\quad +F\Upsilon(x(t)) + \frac{1}{6}\mathcal{B}_u\bar{\Lambda}Km(t) \\ &\quad +\mathcal{B}_u\bar{\Lambda}K\delta(t) + \mathcal{W}\varrho(t)) \\ &\quad +\frac{1}{36}m^T(t)Fm(t) + \frac{1}{36}m^T(t)F\delta(t) \\ &\quad \frac{1}{36}\delta^T(t)Fm(t) + \frac{1}{36}\delta^T(t)F\delta(t)\},\end{aligned}$$

and

$$F = K^T(\Lambda - \bar{\Lambda})^T B^T RB(\Lambda - \bar{\Lambda})K.$$

Utilizing (9) and (18), follows

$$\mathcal{E}\{F\} = \sum_{i=1}^{m}\beta_i^2 K^T\mathcal{C}_i^T B^T RB\mathcal{C}_i K. \quad (20)$$

By Jensen's inequality, we have

$$\int_{t-\varsigma_M}^{t}\dot{x}^T(s)R\dot{x}(s)ds \le \frac{1}{\varsigma_M}\epsilon^T(t)J\epsilon(t), \quad (21)$$

where

$$\epsilon(t) = \begin{bmatrix}x(t) & x(t-\varsigma(t)) & x(t-\varsigma_M)\end{bmatrix},$$
$$J = \begin{bmatrix}-R & * & * \\ R+S & -2R-S-S^T & * \\ -S & R+S & -R\end{bmatrix},$$

combine (19) (20) (21), and by Schur's complement, the result is established. ■

Theorem 2: For given scalars σ, α, γ and ρ, and $\lambda_i (i = 1, \cdots, m)$, $\beta_i (i = 1, \cdots, m)$. The system described by (14) with the feedback gain $K = YX^{-1}$ is globally asymptotically stable in mean square sense if there exist matrices $X > 0, \tilde{Q} > 0, \tilde{\Omega} > 0, \tilde{R} > 0, \tilde{\Omega} > 0$ and $\tilde{S}, Y$ with appropriate dimensions such that

$$\begin{bmatrix}\Psi_{M1} & * \\ \Psi_{M2} & \Psi_{M3}\end{bmatrix} < 0, \quad (22)$$
$$\begin{bmatrix}\tilde{R} & * \\ \tilde{S} & \tilde{R}\end{bmatrix} \ge 0, \quad (23)$$

where

$$\Psi_{M1} = \begin{bmatrix}\Psi_1 & * & * & * \\ \Psi_2 & -\tilde{\Omega} & * & * \\ \Psi_3 & 0 & -\tilde{Q} - \frac{1}{\varsigma_M}\tilde{R} & * \\ \Psi_4 & \sqrt{\varsigma_M}\mathcal{B}_u\bar{\Lambda}Y & 0 & \rho^2\tilde{R} - 2\rho X\end{bmatrix},$$
$$\Psi_{M2} = \begin{bmatrix}\Psi_5 & 0 & 0 & 0 \\ \Psi_6 & \theta' & 0 & 0 \\ \Psi_7 & 0 & 0 & 0\end{bmatrix},$$
$$\Psi_{M3} = \begin{bmatrix}-\alpha^{-2}I & * & * \\ 0 & \hat{R}' & * \\ 0 & 0 & -I\end{bmatrix},$$
$$\Psi_1 = \begin{bmatrix}\psi_1 & * & * & * & * & * \\ F^T & -I & * & * & * & * \\ \psi_2 & 0 & \frac{\sigma}{36}\tilde{\Omega} + \nu' & * & * & * \\ \psi_3 & 0 & \frac{\sigma}{9}\tilde{\Omega} & \frac{4\sigma}{9}\tilde{\Omega} + \nu' & * & * \\ \psi_4 & 0 & \frac{\sigma}{36}\tilde{\Omega} & \frac{\sigma}{9}\tilde{\Omega} & \frac{\sigma}{36}\tilde{\Omega} + \nu' & * \\ \mathcal{W}^T & 0 & 0 & 0 & 0 & -\gamma^2 I\end{bmatrix},$$
$$\Psi_2 = \begin{bmatrix}Y^T\bar{\Lambda}\mathcal{B}_u^T & 0 & 0 & 0 & 0 & 0\end{bmatrix},$$
$$\Psi_3 = \begin{bmatrix}-\frac{1}{\varsigma_M}\tilde{S} & 0 & \frac{1}{\varsigma_M}(\tilde{R}+\tilde{S}) & \frac{1}{\varsigma_M}(\tilde{R}+\tilde{S}) & \frac{1}{\varsigma_M}(\tilde{R}+\tilde{S}) & 0\end{bmatrix},$$
$$\Psi_4 = [\Psi_{41} \quad \Psi_{42}],$$
$$\Psi_{41} = \begin{bmatrix}\sqrt{\varsigma_M}\mathcal{A}X & \sqrt{\varsigma_M}D & \frac{1}{6}\sqrt{\varsigma_M}\mathcal{B}_u\bar{\Lambda}Y\end{bmatrix},$$
$$\Psi_{42} = \begin{bmatrix}\frac{2}{3}\sqrt{\varsigma_M}\mathcal{B}_u\bar{\Lambda}Y & \frac{1}{6}\sqrt{\varsigma_M}\mathcal{B}_u\bar{\Lambda}Y & \sqrt{\varsigma_M}\mathcal{W}\end{bmatrix},$$
$$\Psi_5 = \begin{bmatrix}\mathcal{H} & 0 & 0 & 0 & 0 & 0\end{bmatrix},$$
$$\Psi_6 = \begin{bmatrix}0 & 0 & \theta' & \theta' & \theta' & 0\end{bmatrix},$$
$$\Psi_7 = \begin{bmatrix}I & 0 & 0 & 0 & 0 & 0\end{bmatrix},$$
$$\psi_1 = X\mathcal{A}^T + \mathcal{A}X + \tilde{Q} - \frac{1}{\varsigma_M}\tilde{R},$$
$$\psi_2 = \frac{1}{6}Y^T\bar{\Lambda}^T\mathcal{B}_u^T + \frac{1}{\varsigma_M}(\tilde{R}+\tilde{S}),$$

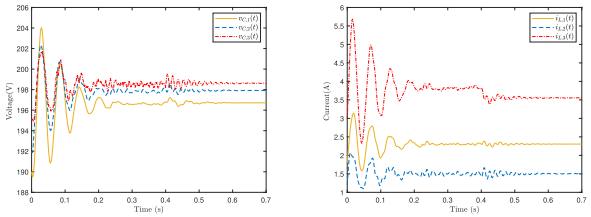

(a) Voltage (b) Current

FIGURE 3. System responses with proposed ETM.

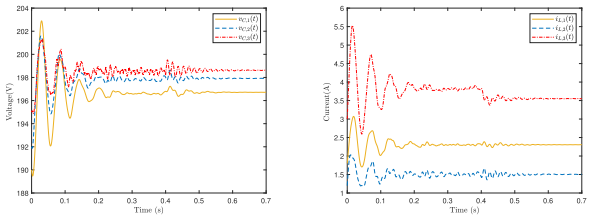

(a) Voltage (b) Current

FIGURE 4. System responses with traditional ETM.

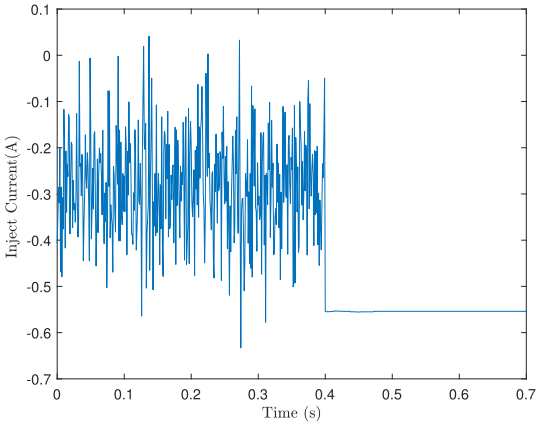

FIGURE 5. Inject current (A).

$$\psi_3 = \frac{2}{3}Y^T\bar{\Lambda}^T\mathcal{B}_u^T + \frac{1}{\varsigma_M}(\tilde{R}+\tilde{S}),$$
$$\psi_4 = \frac{1}{6}Y^T\bar{\Lambda}^T\mathcal{B}_u^T + \frac{1}{\varsigma_M}(\tilde{R}+\tilde{S}),$$
$$\nu' = -\frac{1}{\varsigma_M}(2\tilde{R}+\tilde{S}+\tilde{S}^T),$$
$$\theta' = [\beta_1 B\mathcal{C}_1 Y, \beta_2 B\mathcal{C}_2 Y, \cdots, \beta_m B\mathcal{C}_m Y]^T,$$
$$\hat{R}' = diag\{\underbrace{\tilde{R}, \cdots, \tilde{R}}_{m}\}.$$

Proof: Based on the Theorem 1, post- and pre-multiplying the both sides of (15) with $diag\{X, I, X, X, X, X, I, X, R^{-1}, R^{-1}, I, I\}$ and its transpose, defining $X = P^{-1}$ and $\tilde{Q} = X^TQX, \tilde{\Omega} = X^T\Omega X, \tilde{S} = X^TSX, \tilde{R} = X^TRX$, the (22) can be obtained. The proof is completed. ■

IV. SIMULATION

In this section, a simulation example is given as a verification of the presented control design method for the DC microgrid.

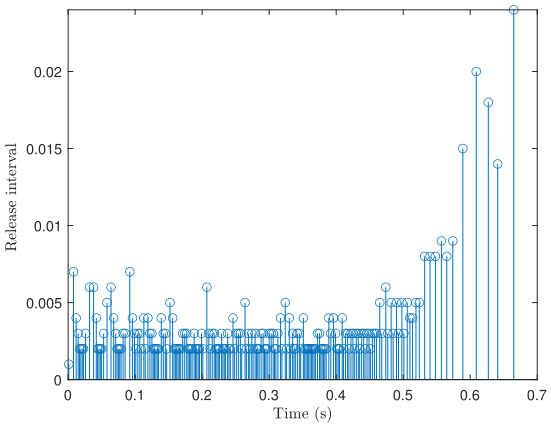

(a) Traditional ETM

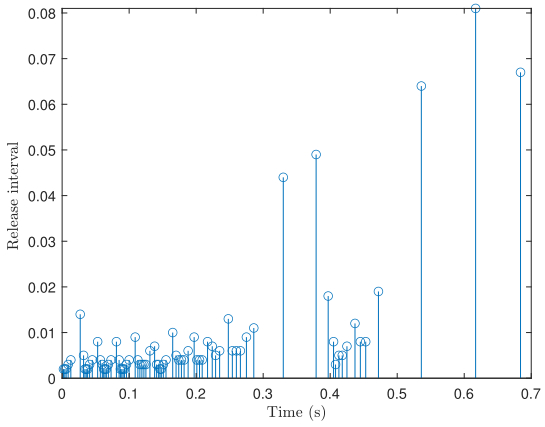

(b) PAETM

FIGURE 6. Triggering event.

This example is a DC microgrid mentioned in [14], [37] and [38] which contains two CPLs and one ESS. The same system parameters of [14] are used in this section. The parameters needed are: $\sigma = 0.05$, $\varsigma_M = 0.001$, $\rho = 0.1$, $\alpha = 0.09$. Selecting the disturbance attenuation level $r = 200$, while the external disturbance $\varrho(t)$ and disturbance matrix $\mathcal{W}$ chosen as follows:

$$\varrho(t) = 30e^{-20t}sin(100t), \tag{24}$$
$$\mathcal{W} = \begin{bmatrix}1 & 1 & 1 & 1 & 1 & 1\end{bmatrix}^T. \tag{25}$$

The actuator faults Λ is obeying a certain probabilistic distribution satisfied $\bar{\Lambda} = 0.5$ and $\beta = 0.2$, which indicate the actuator is experiencing backward gain while having fluctuations in small range. The averaging time is design as $\mathcal{T} = 0.03$, and the initial value of the system x_0 is chosen as:

$$x_0 = [1.80, 190.00, 1.20, 192.00, 3.00, 195.00]^T.$$

In order to gain better performance for this specific system, a restriction to enlarge controller K is considered as follows:

$$\|K\| \geq \mu, \tag{26}$$

where μ is a parameter need to be designed, we set $\mu = 0.046$ here.

From Theorem 2, it has $\|K\| = \|Y\| \|X\|^{-1}$. Then (26) can be rewrite as

$$\mu X^T X - Y^T Y \leq 0. \tag{27}$$

Define a new matrix $\mathcal{N} = Y^T Y$ and apply Schur's complement, there are

$$\begin{bmatrix} -\mathcal{N} & X^T \\ X & -\frac{I}{\mu} \end{bmatrix} \leq 0, \\ \begin{bmatrix} -\mathcal{N} & Y^T \\ Y & -I \end{bmatrix} \leq 0. \tag{28}$$

By solving the Theorem 2 with the inequality (28), the matrix Ω and the feedback gain matrix K of the DC microgrid system are obtained as

$$\Omega = 10^6 \times \begin{bmatrix} \Omega_{11} & \Omega_{12} \\ \Omega_{21} & \Omega_{22} \end{bmatrix},$$
$$\Omega_{11} = \begin{bmatrix} 4.9326 & -0.8863 & 0.0234 \\ -0.8863 & 3.9921 & -0.0008 \\ 0.0234 & -0.0008 & 4.9598 \end{bmatrix},$$
$$\Omega_{12} = \begin{bmatrix} -0.0035 & 0.0022 & -0.0238 \\ 0.0050 & -0.0073 & -0.0171 \\ -0.6546 & 0.0001 & -0.0434 \end{bmatrix},$$
$$\Omega_{21} = \begin{bmatrix} -0.0035 & 0.0050 & -0.6546 \\ 0.0022 & -0.0073 & 0.0001 \\ -0.0238 & -0.0171 & -0.0434 \end{bmatrix},$$
$$\Omega_{22} = \begin{bmatrix} 4.2574 & -0.0055 & -0.0163 \\ -0.0055 & 5.9847 & -0.0020 \\ -0.0163 & -0.0020 & 5.9819 \end{bmatrix},$$
$$K = \begin{bmatrix} K_1 & K_2 \end{bmatrix},$$
$$K_1 = \begin{bmatrix} -0.0467 & -0.0002 & -0.0096 \end{bmatrix},$$
$$K_2 = \begin{bmatrix} 0.0001 & 0.0016 & -0.0096 \end{bmatrix}.$$

Figs. 3 – 6 present the simulation results in $[0, 0.7s]$, in which actuator fault occurs during $[0, 0.4s]$. Fig. 5 stands for the injecting-current which is the control input. The system performance with proposed PAETM is shown in Fig. 3, which indicate that even experiencing probabilistic actuator fault, the multiple nonlinear CPLs involved DC microgrid can still be stabilized. And the system performance with traditional ETM is shown in Fig. 4 by comparing it with Fig. 3, we can reach the conclusion that the system performance under proposed PAETM is still remain acceptable, while Fig. 6 further illustrates the effectiveness of the PAETM, subfigure (a) stands for the triggering event of the system with traditional mechanism, which has much more dense triggering events, especially when the actuator fault and disturbance occur, those extra triggering events cause much more energy consumption for ESS and rise the possibility of firmware damaging. Moreover, it occupies the network which may lead to system unstable. While subfigure (b) stands for the system with the proposed average mechanism, it reduces non-essential triggering events while maintaining the system performance in certain degree. The data releasing rates between those two different cases are listed in the table 1.

TABLE 1. Releasing differences between two cases.

Cases	Normal	Improved
Total sampling	700	700
Total releasing	191	87
Releasing rate	27.29%	12.43%

It's obviously that, by using the proposed averaging mechanism, the data releasing rate drops 14.86% while the control performance remain acceptable.

The simulation result indicates that (i) The nonlinear CPLs involved DC Microgrid system are stable under the proposed control mechanism while the system experience external disturbance and uncertain actuator faults; (ii) By applying the proposed improvement, the triggering events are reduced while the system performance remains a certain level, which indicates the effectiveness of the proposed event-triggered mechanism on both saving network bandwidth and energy.

V. CONCLUSION

In this paper, a novel event-triggered control scheme design approach for DC microgrid system with actuator faults is proposed. This novel ETM can further reduce unnecessary triggering events. A practical actuator fault obeying certain distribution is taken into consideration. By utilizing Lyapunov stability theory and LMI method, the event-triggered controller has been designed. Furthermore, by introducing the averaging mechanism before the sampling, the average value of each sample interval has been obtained and used to evaluate the triggering condition. Benefit from this improvement, the quantity of triggering is reduced while the system performance is guaranteed. In the end, to verify the proposed control scheme for nonlinear DC microgrid system can stabilize the system and to illustrate the effectiveness of the proposed ETM, a simulation is given. For further study, the event-triggered fault diagnosis for DC microgrids with nonlinearities may worth deep investigation.

REFERENCES

[1] T. Dragičević, X. Lu, J. C. Vasquez, and J. M. Guerrero, "DC microgrids—Part I: A review of control strategies and stabilization techniques," *IEEE Trans. Power Electron.*, vol. 31, no. 7, pp. 4876–4891, Jul. 2016.
[2] J. Zhou, Y. Xu, H. Sun, Y. Li, and M.-Y. Chow, "Distributed power management for networked AC–DC microgrids with unbalanced microgrids," *IEEE Trans. Ind. Informat.*, vol. 16, no. 3, pp. 1655–1667, Mar. 2020.
[3] X. Zhang, F. Yang, and X. Sun, "Resilient adaptive event-triggered load frequency control of network-based power systems against deception attacks," *Sensors*, vol. 21, no. 21, p. 7047, Oct. 2021.
[4] J. Cao, Z. Bu, Y. Y. Wang, H. Yang, J. C. Jiang, and H. J. Li, "Detecting prosumer-community groups in smart grids from the multiagent perspective," *IEEE Trans. Syst., Man, Cybern., Syst.*, vol. 49, no. 8, pp. 1652–1664, Aug. 2019.
[5] Q. Xu, C. Zhang, C. Wen, and P. Wang, "A novel composite nonlinear controller for stabilization of constant power load in DC microgrid," *IEEE Trans. Smart Grid*, vol. 10, no. 1, pp. 752–761, Jan. 2019.

[6] M.-H. Khooban, T. Dragičević, F. Blaabjerg, and M. Delimar, "Shipboard microgrids: A novel approach to load frequency control," *IEEE Trans. Sustain. Energy*, vol. 9, no. 2, pp. 843–852, Apr. 2018.

[7] A. Kwasinski and C. N. Onwuchekwa, "Dynamic behavior and stabilization of DC microgrids with instantaneous constant-power loads," *IEEE Trans. Power Electron.*, vol. 26, no. 3, pp. 822–834, Mar. 2011.

[8] T. Dragičević, "Dynamic stabilization of DC microgrids with predictive control of point-of-load converters," *IEEE Trans. Power Electron.*, vol. 33, no. 12, pp. 10872–10884, Dec. 2018.

[9] S. A. G. K. Abadi, S. I. Habibi, T. Khalili, and A. Bidram, "A model predictive control strategy for performance improvement of hybrid energy storage systems in DC microgrids," *IEEE Access*, vol. 10, pp. 25400–25421, 2022.

[10] X. Lu, K. Sun, J. M. Guerrero, J. C. Vasquez, L. Huang, and J. Wang, "Stability enhancement based on virtual impedance for DC microgrids with constant power loads," *IEEE Trans. Smart Grid*, vol. 6, no. 6, pp. 2770–2783, Nov. 2015.

[11] M. Wu and D. D.-C. Lu, "A novel stabilization method of LC input filter with constant power loads without load performance compromise in DC microgrids," *IEEE Trans. Ind. Electron.*, vol. 62, no. 7, pp. 4552–4562, Jul. 2015.

[12] P. Magne, B. Nahid-Mobarakeh, and S. Pierfederici, "General active global stabilization of multiloads DC-power networks," *IEEE Trans. Power Electron.*, vol. 27, no. 4, pp. 1788–1798, Apr. 2012.

[13] M. Zhang, Y. Li, F. Liu, L. Luo, Y. Cao, and M. Shahidehpour, "Voltage stability analysis and sliding-mode control method for rectifier in DC systems with constant power loads," *IEEE Trans. Emerg. Sel. Topics Power Electron.*, vol. 5, no. 4, pp. 1621–1630, Dec. 2017.

[14] L. Herrera, W. Zhang, and J. Wang, "Stability analysis and controller design of DC microgrids with constant power loads," *IEEE Trans. Smart Grid*, vol. 8, no. 2, pp. 881–888, Mar. 2017.

[15] L. Ding, Q.-L. Han, L. Y. Wang, and E. Sindi, "Distributed cooperative optimal control of DC microgrids with communication delays," *IEEE Trans. Ind. Informat.*, vol. 14, no. 9, pp. 3924–3935, Sep. 2018.

[16] J. Kumar, A. Agarwal, and V. Agarwal, "A review on overall control of DC microgrids," *J. Energy Storage*, vol. 21, pp. 113–138, Feb. 2019.

[17] V. Nasirian, S. Moayedi, A. Davoudi, and F. L. Lewis, "Distributed cooperative control of DC microgrids," *IEEE Trans. Power Electron.*, vol. 30, no. 4, pp. 2288–2303, Apr. 2015.

[18] M. Cucuzzella, S. Trip, C. De Persis, X. Cheng, A. Ferrara, and A. van der Schaft, "A robust consensus algorithm for current sharing and voltage regulation in DC microgrids," *IEEE Trans. Control Syst. Technol.*, vol. 27, no. 4, pp. 1583–1595, Jul. 2019.

[19] R. Ma, H.-H. Chen, Y.-R. Huang, and W. Meng, "Smart grid communication: Its challenges and opportunities," *IEEE Trans. Smart Grid*, vol. 4, no. 1, pp. 36–46, Mar. 2013.

[20] X. Zhang, Q.-L. Han, X. Ge, D. Ding, L. Ding, D. Yue, and C. Peng, "Networked control systems: A survey of trends and techniques," *IEEE/CAA J. Autom. Sinica*, vol. 7, no. 1, pp. 1–17, Jun. 2020.

[21] J. Cao, D. Ding, J. Liu, E. Tian, S. Hu, and X. Xie, "Hybrid-triggered-based security controller design for networked control system under multiple cyber attacks," *Inf. Sci.*, vol. 548, pp. 69–84, Feb. 2021.

[22] Z. Gu, S. Yan, C. K. Ahn, D. Yue, and X. Xie, "Event-triggered dissipative tracking control of networked control systems with distributed communication delay," *IEEE Syst. J.*, vol. 16, no. 2, pp. 3320–3330, Jun. 2022.

[23] X. Mu, Z. Gu, and L. Hua, "Memory-based event-triggered leader-following consensus for T-S fuzzy multi-agent systems subject to deception attacks," *J. Franklin Inst.*, vol. 359, no. 1, pp. 599–618, Jan. 2022.

[24] Z. Gu, C. K. Ahn, D. Yue, and X. Xie, "Event-triggered H_∞ filtering for T–S fuzzy-model-based nonlinear networked systems with multisensors against DoS attacks," *IEEE Trans. Cybern.*, vol. 52, no. 6, pp. 5311–5321, Jun. 2022.

[25] Z. Wu, J. Cao, Y. Wang, Y. Wang, L. Zhang, and J. Wu, "HPSD: A hybrid PU-learning-based spammer detection model for product reviews," *IEEE Trans. Cybern.*, vol. 50, no. 4, pp. 1595–1606, Apr. 2020.

[26] T. Yin and Z. Gu, "Security control for adaptive event-triggered networked control systems under deception attacks," *IEEE Access*, vol. 9, pp. 10789–10796, 2021.

[27] L. Xing, C. Wen, Z. Liu, H. Su, and J. Cai, "Event-triggered output feedback control for a class of uncertain nonlinear systems," *IEEE Trans. Autom. Control*, vol. 64, no. 1, pp. 290–297, Jan. 2019.

[28] L. Xing, Y. Mishra, Y.-C. Tian, G. Ledwich, C. Zhou, W. Du, and F. Qian, "Distributed state-of-charge balance control with event-triggered signal transmissions for multiple energy storage systems in smart grid," *IEEE Trans. Syst., Man, Cybern. Syst.*, vol. 49, no. 8, pp. 1601–1611, Aug. 2019.

[29] X. Mu and S. Yan, "Adaptive leader-following consensus tracking control of multiple UAVs subject to deception attacks," *Processes*, vol. 10, no. 4, p. 757, Apr. 2022.

[30] S. Sahoo and S. Mishra, "An adaptive event-triggered communication-based distributed secondary control for DC microgrids," *IEEE Trans. Smart Grid*, vol. 9, no. 6, pp. 6674–6683, Nov. 2018.

[31] D. Pullaguram, S. Mishra, and N. Senroy, "Event-triggered communication based distributed control scheme for DC microgrid," *IEEE Trans. Power Syst.*, vol. 33, no. 5, pp. 5583–5593, Sep. 2018.

[32] V. Kumar, S. R. Mohanty, and S. Kumar, "Event trigger super twisting sliding mode control for DC micro grid with matched/unmatched disturbance observer," *IEEE Trans. Smart Grid*, vol. 11, no. 5, pp. 3837–3849, Sep. 2020.

[33] X. Wang and M. D. Lemmon, "Self-triggered feedback control systems with finite-gain $\mathcal{L}_2$ stability," *IEEE Trans. Autom. Control*, vol. 54, no. 3, pp. 452–467, Mar. 2009.

[34] A. Anta and P. Tabuada, "To sample or not to sample: Self-triggered control for nonlinear systems," *IEEE Trans. Autom. Control*, vol. 55, no. 9, pp. 2030–2042, Sep. 2010.

[35] Q. Li, B. Shen, Z. Wang, T. Huang, and J. Luo, "Synchronization control for a class of discrete time-delay complex dynamical networks: A dynamic event-triggered approach," *IEEE Trans. Cybern.*, vol. 49, no. 5, pp. 1979–1986, May 2019.

[36] Z. Gu, X. Sun, H.-K. Lam, D. Yue, and X. Xie, "Event-based secure control of T–S fuzzy-based 5-DOF active semivehicle suspension systems subject to DoS attacks," *IEEE Trans. Fuzzy Syst.*, vol. 30, no. 6, pp. 2032–2043, Jun. 2022.

[37] S. Hu, P. Yuan, D. Yue, C. Dou, Z. Cheng, and Y. Zhang, "Attack-resilient event-triggered controller design of DC microgrids under DoS attacks," *IEEE Trans. Circuits Syst. I, Reg. Papers*, vol. 67, no. 2, pp. 699–710, Feb. 2020.

[38] M. A. Kardan, M. H. Asemani, A. Khayatian, N. Vafamand, M. H. Khooban, T. Dragičević, and F. Blaabjerg, "Improved stabilization of nonlinear DC microgrids: Cubature Kalman filter approach," *IEEE Trans. Ind. Appl.*, vol. 54, no. 5, pp. 5104–5112, Sep. 2018.

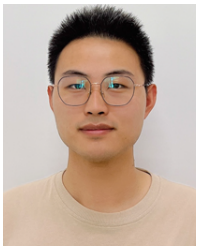

BOWEI JI received the B.E. degree in automation from Nanjing Forestry University, Nanjing, China, in 2020, where he is currently pursuing the M.E degree with the School of Mechanical and Electronic Engineering. His research interests include networked control systems and smart grid.

ZHOU GU (Member, IEEE) received the B.S. degree from North China Electric Power University, Beijing, China, in 1997, and the M.S. and Ph.D. degrees in control science and engineering from the Nanjing University of Aeronautics and Astronautics, Nanjing, China, in 2007 and 2010, respectively. From September 1996 to January 2013, he was an Associate Professor with the School of Power Engineering, Nanjing Normal University. He was a Visiting Scholar with Central Queensland University, Rockhampton, QLD, Australia, and The University of Manchester, Manchester, U.K. He is currently a Professor with Nanjing Forestry University, Nanjing. His current research interests include networked control systems, time-delay systems, and reliable control and their applications.

XIUFENG MU received the B.S. degree from Nanjing Forestry University, Nanjing, China, in 2013, where he is currently pursuing the Ph.D. degree. His research interests include networked control systems, UAV consensus control, multi-agent systems, and time-delay systems.